Title

Splicing inactivation generates hybrid mRNA-snoRNA transcripts targeted by cytoplasmic RNA decay

Journal

Proceedings of the National Academy of Sciences of the United States of America, 119(31)

ISSN

0027-8424

Authors

Liu, Yanru
DeMario, Samuel
He, Kevin
et al.

Publication Date

2022-08-02

DOI

10.1073/pnas.2202473119

Peer reviewed

PNAS RESEARCH ARTICLE | BIOCHEMISTRY OPEN ACCESS

Splicing inactivation generates hybrid mRNA-snoRNA transcripts targeted by cytoplasmic RNA decay

Yanru Liu[a,1,2], Samuel DeMario[a,1], Kevin He[a], Michelle R. Gibbs[a], Keaton W. Barr[a], and Guillaume F. Chanfreau[a,b,3]

Edited by Joan Steitz, Yale University, New Haven, CT; received February 10, 2022; accepted June 14, 2022

Many small nucleolar RNAs (snoRNA)s are processed from introns of host genes, but the importance of splicing for proper biogenesis and the fate of the snoRNAs is not well understood. Here, we show that inactivation of splicing factors or mutation of splicing signals leads to the accumulation of partially processed hybrid messenger RNA–snoRNA (hmsnoRNA) transcripts. hmsnoRNAs are processed to the mature 3′ ends of the snoRNAs by the nuclear exosome and bound by small nucleolar ribonucleoproteins. hmsnoRNAs are unaffected by translation-coupled RNA quality-control pathways, but they are degraded by the major cytoplasmic exonuclease Xrn1p, due to their messenger RNA (mRNA)-like 5′ extensions. These results show that completion of splicing is required to promote complete and accurate processing of intron-encoded snoRNAs and that splicing defects lead to degradation of hybrid mRNA-snoRNA species by cytoplasmic decay, underscoring the importance of splicing for the biogenesis of intron-encoded snoRNAs.

snoRNA | splicing | introns | exosome | exonuclease

Significance

Small nucleolar RNAs (snoRNAs) mediate modifications of nucleosides within ribosomal RNAs, which are necessary for proper ribosomal function and translation. Many snoRNAs are encoded within introns of host genes, and accurate biogenesis of these small RNAs is required to produce functional snoRNAs. The work presented here shows that when the splicing reactions are inactivated, snoRNAs undergo a distinct biogenesis pathway, which leads to the production of aberrant hybrid RNAs that contain both messenger RNA (mRNA) and small RNA components of the host genes. While snoRNAs are primarily found in the nucleolus, these hybrid RNAs are degraded by the cytoplasmic mRNA degradation pathway. These results demonstrate the importance of splicing to promote accurate snoRNA processing and prevent the production of aberrant mRNA-snoRNA hybrids.

Small nucleolar RNAs (snoRNAs) are noncoding RNAs that guide small nucleolar ribonucleoprotein (snoRNP)-mediated 2′-O-methylation or pseudouridylation of pre-ribosomal RNA precursors and other stable RNAs (1–3). These snoRNAs are classified in two major families: the C/D and H/ACA classes, which guide 2′-O-methylation and pseudouridylation of their substrates, respectively. The importance of correct snoRNA expression is underscored by the fact that defects in snoRNA metabolism are linked to multiple pathologic processes, including cancer (4, 5), Prader-Willi syndrome (6), and metabolic stress (7). snoRNAs are found in many different genomic contexts (2, 8). In mammalian genomes, many snoRNAs are present in the introns of host genes, but they can also be generated from long noncoding RNAs (lncRNAs). In plants, snoRNAs are often generated from polycistronic transcription units (8). In the budding yeast *Saccharomyces cerevisiae*, which has been used extensively to study the mechanisms of snoRNA biogenesis and processing, snoRNAs are expressed either from independently transcribed genes, polycistronic snoRNA precursors, or from introns (2, 8). The synthesis of mature snoRNAs from intronic sequences is thought to occur primarily through splicing of the host gene precursor messenger RNA (pre-mRNA). In vitro and in vivo studies have shown that splicing results in accurate processing of intron-encoded snoRNA in mammalian cells (9). The current model is that intron-encoded snoRNAs are generated by exonucleolytic trimming of the excised linear introns after completion of the splicing reaction and debranching of the lariat introns. In support of this model, inactivation of the *S. cerevisiae* debranching enzyme Dbr1p results in the accumulation of lariat intron species containing the snoRNAs (10), showing that debranching of the excised intron is critical for processing. However, the production of mature snoRNA can still occur inefficiently in the absence of the debranching enzyme (10), because random hydrolytic cleavage of the lariat intron exposes the cleaved intron to processing by exonucleases, or through cleavage by the RNase III enzyme Rnt1p (11). In addition, some studies have reported splicing-independent processing of intron-encoded snoRNAs (12), either by endonucleolytic cleavage of the precursors (11, 13) or by exonucleolytic processing (14). In *S. cerevisiae*, the Rnase P endonuclease has also been proposed to initiate a processing pathway independent from splicing, by cleaving unspliced pre-mRNAs that host box C/D snoRNAs (15). Finally, snoRNAs can be found associated with stable lariats (16), and processing of introns containing multiple snoRNAs can generate sno-lncRNAs, which correspond to partially processed introns that contain two snoRNAs linked by an intronic segment (17).

Despite the known importance of splicing for the processing of intron-encoded snoRNAs, it is unclear how defects in the spliceosome machinery may impact the fate of intron-encoded snoRNAs. This is an important question, as recent work has shown that defects in 5′-end processing of independently transcribed snoRNAs can result in

Author contributions: S.D. and G.F.C. designed research; Y.L., S.D., K.H., M.R.G., and K.W.B. performed research; S.D., K.H., and G.F.C. analyzed data; and G.F.C. wrote the paper.

The authors declare no competing interest.

This article is a PNAS Direct Submission.

[1]Y.L. and S.D. contributed equally to this work.

[2]Present address: Department of Molecular Biology and Genetics, Cornell University, Ithaca, NY 14853-2703.

[3]To whom correspondence may be addressed. Email: guillom@chem.ucla.edu.

This article contains supporting information online at http://www.pnas.org/lookup/suppl/doi:10.1073/pnas.2202473119/-/DCSupplemental.

Published July 25, 2022.

mis-localization of the unprocessed snoRNAs in budding yeast (18). Strikingly, very little is known about the impact of spliceosome defects on snoRNA expression. Haploinsufficiency of the core small nuclear ribonucleoprotein (snRNP) SmD3 results in a reduction in the levels of intron-encoded snoRNAs (19), but the specific molecular effects of this mutation on the biogenesis pathway of intron-encoded snoRNAs have not been investigated. In this study, we have analyzed the impact of inactivating splicing using trans- and cis-acting splicing mutants on the production of intron-encoded snoRNAs in the yeast *S. cerevisiae*. We show that inactivating splicing factors involved in different steps of the spliceosome cycle or mutating the splicing signal of a host gene result in the accumulation of aberrant, hybrid mRNA-snoRNAs species, which share some of the hallmarks of mature snoRNAs but are degraded by the cytoplasmic decay. These results highlight the importance of splicing for determining the fate of intron-encoded snoRNAs and show that incorrectly processed intron-encoded snoRNAs are degraded by the general messenger RNA (mRNA) decay pathway. Our results may also provide some insights into possible additional effects of genetic diseases that affect splicing factors.

Results

Inactivation of Splicing Factors at Different Stages of the Cycle Results in the Accumulation of Hybrid mRNA-snoRNA Forms of *NOG2/snR191*. To investigate the importance of the splicing reaction for the processing of intron-encoded snoRNAs, we used the anchor away (AA) technique (20), which promotes the rapid export of endogenously FRB (*FKBP12*-rapamycin binding domain)-tagged splicing factors to the cytoplasm after addition of rapamycin (20). This results in the nuclear depletion of these factors and in the inactivation of their nuclear functions in vivo. The genetic background used for these experiments alleviates the toxic effects of rapamycin and its downstream effects on gene regulation (20). To analyze the contribution of splicing factors involved at different steps of the spliceosome cycle, we used strains expressing FRB-tagged versions of Prp5p, Prp28p, Prp16p, Prp18p, Slu7p, and Prp22p. These proteins are involved in various steps of splicing (21), from spliceosome assembly (Prp5p, Prp28p) to the second catalytic step (Prp16p, Prp18p, Slu7p, Prp22p) and spliceosome recycling (Prp22p). We first analyzed expression of the *NOG2* gene, which contains the H/ACA snoRNA snR191 in its intron (22), by Northern blot (Fig. 1*A*). After nuclear depletion of each of these splicing factors, a probe hybridizing to the first exon of *NOG2* detected the unspliced precursors but also RNAs migrating faster than the spliced mRNAs (labeled "hms" in Fig. 1*B*). hmsRNAs were detected in all the AA strains treated with rapamycin but not prior to rapamycin treatment. We first hypothesized that these species might correspond to cleaved 5′ exons; however, based on their estimated size (~1100 nucleotides [nt]), these species are too large to correspond to free 5′ exons. In addition, these RNAs were also detected after anchoring away proteins involved prior to the first catalytic step (e.g., Prp5p, Prp28p). Furthermore, species migrating faster than the hms RNAs and whose size matched those of cleaved 5′ exons (~850 nt) were detected only in strains in which second-step splicing factors are anchored away (i.e., Slu7p, Prp16p, Prp18p, Prp22p), but not in strains in which splicing factors involved prior to the first step are depleted from the nucleus (i.e., Prp5p, Prp28p). These fastest migrating species correspond to cleaved 5′ exons that fail to undergo splicing because of second-step defects and are labeled "E1" in all figures.

Further mapping of the hms RNAs, using probes hybridizing to the different regions of the *NOG2-snR191* gene (Fig. 1*A*), showed that these species also hybridize to probes complementary to the mature snR191 snoRNA and to the intronic region preceding the snoRNA (Fig. 1*C*). Based on their approximate size (~1100 nt) and their hybridization patterns, we hypothesized that these RNAs correspond to hybrid mRNA-snoRNA (hmsnoRNA) containing the mRNA 5′ exon, the intronic segment upstream of the snoRNA, and the entire snoRNA sequence (schematic representation is shown in Fig. 1*A*). The combination of estimated sizes and probe hybridization patterns was consistent with a 3′ end close to that of the mature snoRNA 3′ end. To test this idea, we mapped the 3′ end of the *NOG2-snR191* hmsnoRNA using a modified 3′–Rapid Amplification of cDNA Ends (RACE) protocol after in vitro polyadenylation of total RNAs. Sequencing of the 3′-RACE products showed that the *snR191* hmsnoRNA 3′ ends match precisely those of mature snoRNAs (*SI Appendix*, Fig. S1). RNAs similar in size to the hms species also accumulated in mutants carrying deletions of the nonessential genes encoding the U2 snRNP component Lea1p (23) or the splicing fidelity factor Isy1p (24) (Fig. 1*D*). Therefore, the production of hmsnoRNAs is caused by general splicing defects rather than by indirect effects of the AA process.

HmsnoRNAs Can Be Detected for Most Intron-Encoded *S. cerevisiae* snoRNAs by Northern Blot and Nanopore Long-Read Sequencing. To extend the results described above for other snoRNAs, we analyzed RNAs accumulating in the Slu7p-AA strain prior to or after rapamycin treatment for several genes expressing box C/D snoRNAs from their introns: *IMD4*/*snR54* (Fig. 1*E*), *TEF4*/*snR38* (Fig. 1*F*), and *ASC1*/snR24 (*SI Appendix*, Fig. S2). For *IMD4*/*snR54* and *TEF4*/*snR38*, we detected the accumulation of hmsnoRNAs hybridizing to both exon 1 and snoRNA probes (Fig. 1 *E* and *F*). Mapping of the *ASC1*/*snR24* hmsnoRNA using four probes hybridizing to different regions of *ASC1* (*SI Appendix*, Fig. S2 *A* and *B*) showed that these species contain the first exon of *ASC1*, the first part of the intron, and the entire snoRNA sequence that ends close to the mature 3′ end (*SI Appendix*, Fig. S2 *A* and *B*). The estimated size and hybridization patterns of the *IMD4*/*snR54* and *TEF4*/*snR38* hmsnoRNAs (Fig. 1 *E* and *F*) suggest a similar architecture. Mapping of the 3′ end of the *IMD4*/*snR54* hmsnoRNA using the modified 3′-RACE protocol showed that the *IMD4*/*snR54* hmsnoRNA 3′ end is identical to that of the mature *snR54* (*SI Appendix*, Fig. S1). Thus, splicing inactivation results in the general accumulation of hybrid mRNA-snoRNA species for all intron-encoded snoRNAs tested, which belong to both H/ACA and C/D families.

To perform a more comprehensive mapping of hmsnoRNA genome-wide, we performed a direct RNA long-read sequencing experiment on RNAs extracted from an Slu7-AA strain after addition of rapamycin, using the Oxford Nanopore platform. Prior analysis revealed that the majority of the *ASC1*/*snR24* hmsnoRNAs are not polyadenylated (*SI Appendix*, Fig. S2*C*), so the standard protocol to perform direct poly(A)+ RNA sequencing could not be used. We developed a protocol that used in vitro polyadenylation after ribosomal RNA (rRNA) depletion, which allowed detection of the hmsnoRNA by Nanopore sequencing. In the strain in which Slu7p was anchored away, hmsnoRNAs could be detected for *EFB1-snR18* (Fig. 2*A*), *ASC1-snR24* (Fig. 2*B*), *TEF4-snR38* (Fig. 2*C*), *IMD4-snR54* (Fig. 2*D*), *RPL7A-snR39* (Fig. 2*E*), *NOG2-snR191* (Fig. 2*F*), and *RPL7B-snR59* (*SI Appendix*, Fig. S3*A*). The architecture of hmsnoRNAs revealed by long-read sequencing matched perfectly the predictions made above

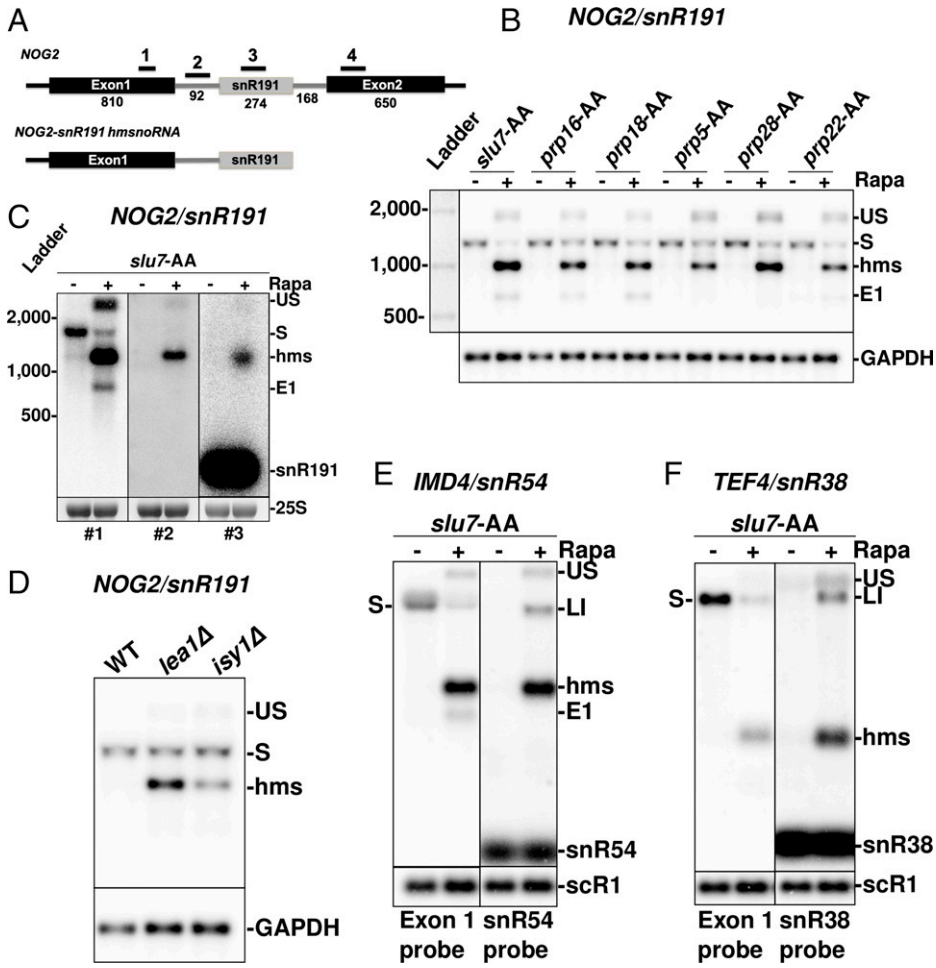

Fig. 1. Hybrid forms of intron-encoded snoRNAs are produced upon splicing inactivation. (*A*) Schematic structure of the *NOG2* gene encoding the *snR191* H/ACA snoRNA in its intron, and proposed structure of the *NOG2-snR191* hmsnoRNA. Exons are represented by black boxes and the mature snoRNA by a gray box. Intronic sequences are shown as gray lines. Numbers indicate the length, in nts, of the different exonic and intronic regions and of the snoRNA. UTR lengths are not included. Black lines with numbers 1 to 3 indicate the approximate locations of the different riboprobes used for this figure. Boxes and line lengths are not to scale. (*B*) Northern blot analysis of *NOG2/snR191* in strains expressing AA FRB-tagged versions of the Slu7p, Prp16p, Prp18p, Prp5p, Prp28p, and Prp22p splicing factors. Each FRB-tagged strain was grown in normal medium and then spun down and resuspended in either fresh normal medium or shifted to medium containing rapamycin (Rapa) for 1 h to promote export of the tagged splicing factor out of the nucleus. (Top) Probe 1 was used. GAPDH was used as a loading control. ; (*C*) Mapping of the hmsnoRNA forms of *snR191* using different riboprobes. Shown are Northern blots of *NOG2/snR191* using riboprobes 1, 2, and 3 shown in panel *A* of RNAs extracted from the Slu7-AA strain before or after 1 h of treatment with rapamycin. An ethidium bromide staining of the 25S rRNA is shown as a loading control. (*D*) Wild-type (WT) Northern blot analysis of *NOG2* in strains in WT and *lea1*Δ or *isy1*Δ deletion strains. (*E*) Northern blot analysis of *IMD4/snR54* in RNAs extracted from the Slu7p-AA strain before or after treatment with rapamycin for 1 h. Shown are Northern blots using probes hybridizing to the 5′ exon or to the mature snoRNA. Labeling of the different species is as in *B*. *scR1* was used as a loading control. (*F*) Northern blot analysis of *TEF4/snR38* in the Slu7p-AA strain. E1, cleaved 5′exon; LI, lariat intron-exon 2 intermediate; S, spliced mRNA; US, unspliced pre-mRNA.

using Northern blot and confirmed that these species contain the 5′ exon, the beginning of the intron, and the snoRNA up the mature 3′ ends. We also detected unspliced precursors and cleaved 5′ exons that accumulate due to the second-step splicing defect (Fig. 2). We did not detect any hmsnoRNA for the *RPS22B-snR44* gene (*SI Appendix*, Fig. S3*B*), likely because of the presence of an RNase III cleavage site in the first intron of the unspliced precursors, which precludes the accumulation of exon1-intron1-exon2-snR44 species when unspliced species are generated (25). Our sequencing approach produced many reads for the box H/ACA *snR191* (Fig. 2*F*) but failed to detect most mature box C/D snoRNA, with the exception of a few reads for *snR18* (Fig. 2*A*).This lack of detection may be linked to the small size of box C/D snoRNAs, which makes their mapping challenging by Oxford Nanopore sequencing. Overall, these results show that after splicing inactivation, hmsnoRNAs are generated from most intron-encoded snoRNAs in *S. cerevisiae*, and the reads obtained confirmed the general architecture of these RNAs.

HmsnoRNAs Are Processed at Their 3′ Ends by Exonucleolytic Trimming by the Exosome. The previous results using 3′-RACE and Nanopore sequencing showed that the 3′ ends of hmsnoRNAs are identical to those of mature snoRNAs, which are generated by exonucleolytic trimming by the nuclear exosome (26). To test the hypothesis that hmsnoRNAs acquire their 3′ end through exosome-mediated processing, we used an AA strain in which the nuclear exosome component Rrp6p is FRB tagged. Anchoring away Rrp6p provides a more effective method of inactivating the nuclear exosome than deleting the gene encoding Rrp6p (27), possibly because exporting Rrp6p to the cytoplasm may also result in the nuclear depletion of other nuclear-exosome components. We then generated a strain in which Rrp6p and Prp18p or Slu7p could be coanchored away simultaneously. Nuclear depletion of Rrp6p resulted in an increased accumulation of both the unspliced and spliced forms of *NOG2* (Fig. 3*A*). This observation is consistent with previous studies that showed that the nuclear exosome actively degrades unspliced precursors and may limit the

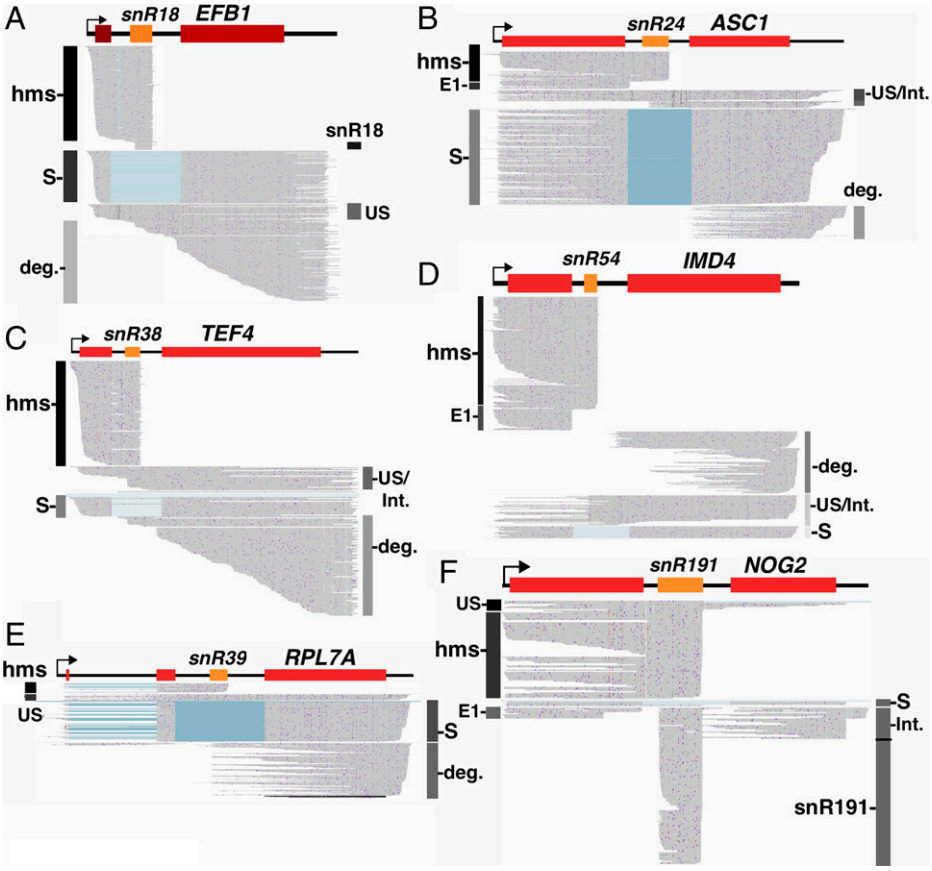

Fig. 2. Detection of hmsnoRNAs by direct single-molecule Oxford Nanopore RNA sequencing. For all the panels, each sequencing read is represented by a horizontal gray line. RNA species are labeled as follows: US, unspliced pre-mRNA; S, spliced mRNA; E1, cleaved 5′ exon; deg., degradation intermediates; Int., snoRNA processing intermediates. (*A–F*) Oxford Nanopore sequencing reads obtained from a *slu7*-FRB–tagged strain treated for 1 h with rapamycin for the following loci: (*A*) *EFB1-snR18* ; (*B*) *ASC1-snR24;* (*C*) *TEF4-snR38;* (*D*) *IMD4-snR54; RPL7A-snR39; and* (*F*) *NOG2-snR191*.

production of mature species (28–30). Hybridization with a probe complementary to snR191 detected the accumulation of shortly extended forms of snR191 in the Rrp6p-AA strain (*SI Appendix*, Fig. S4), consistent with the known role of the exosome in trimming intronic snoRNA mature 3′ ends (26).

As shown previously, anchoring away Slu7p (Fig. 3*A* and *SI Appendix*, Fig. S4) or Prp18p (Fig. 3*A*), resulted in the accumulation of *NOG2-snR191* hmsnoRNAs. Strikingly, when Rrp6p was anchored away simultaneously with Prp18p or Slu7p, the accumulation of the hmsnoRNA decreased compared with what was observed when anchoring away these splicing factors alone (Fig. 3*A*; see also *SI Appendix*, Fig. S4 for Slu7p). Similar results were obtained for *ASC1-snR24* (Fig. 3*B*). We observed a concomitant increase in the level of unspliced precursors (Fig. 3*A* and *SI Appendix*, Fig. S4). These results suggested a precursor-to-product relationship between unspliced pre-mRNAs and hmsnoRNAs, and that hmsnoRNAs are generated by exonucleolytic trimming of unspliced precursors by the nuclear exosome.

To further demonstrate that hmsnoRNAs are processed to or near the 3′ ends of the mature snoRNAs by the exosome, we used strains in which the gene encoding the nonessential U2 snRNP component Lea1p is deleted, along with a deletion of the gene encoding Rrp6p. Consistent with the results obtained above, the *rrp6*Δ knockout resulted in a reduction in the accumulation of *NOG2-snR191* hmsnoRNA species when coupled to the *lea1*Δ mutation, accompanied by an accumulation of unspliced precursors (Fig. 3*C*). Overall, these results, combined with the analyses described above, show that hmsnoRNAs are processed by the nuclear exosome to generate 3′ ends identical to those of the corresponding mature snoRNAs.

HmsnoRNAs Are Not Targeted by Translation-Dependent Quality-Control Pathways. Because hmsnoRNAs contain 5′-untranslated region (UTR) and exon 1 sequences, they exhibit mRNA-like features at their 5′ ends, which suggests that they might be translated. However, they lack a poly(A) tail, which may limit translation efficiency. If hmsnoRNAs are translated, translation would stop shortly after the end of the 5′-exon sequence because of the occurrence of premature stop codons in the intronic sequences, which may trigger nonsense-mediated decay (NMD). NMD could potentially affect hmsnoRNAs, since NMD can occur in the absence of a poly(A) tail in yeast (31). Alternatively, the presence of secondary structures in the snoRNAs or the binding by snoRNPs (see below) may block ribosome progression and trigger No-Go Decay (32). To investigate a potential targeting of hmsnoRNAs by these two RNA surveillance pathways, we knocked out the genes encoding the NMD factor Upf1p or the No-Go Decay factor Dom34p in the *lea1*Δ mutant and analyzed *NOG2-snR191* and *IMD4-snR54* by Northern blot (Fig. 3*C* and *D*). Eliminating Upf1p or Dom34p did not increase the levels of hmsnoRNAs in the *lea1*Δ mutant (Fig. 3*C* and *D*). Instead, the *upf1*Δ knockout resulted in a decrease of the level of hmsoRNAs, while eliminating Dom34p showed no effect. As opposed to what was observed in the *lea1*Δ*rrp6*Δ mutant, the decreased accumulation of the *NOG2-snR191* hmsnoRNA detected in the *lea1*Δ*upf1*Δ mutant did not

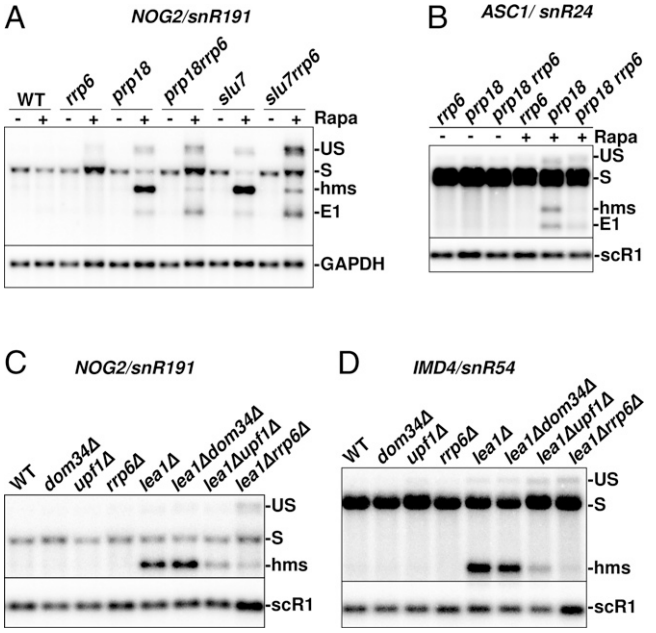

Fig. 3. hmsnoRNAs acquire their 3′ ends through processing by the nuclear exosome but are mostly unaffected by cytoplasmic quality-control pathways. (*A*) Northern blot analysis of *NOG2/snR191* in strains expressing FRB-tagged, AA versions of Rrp6p, Prp18p, Slu7p, or double AA versions. Strains in the name of the gene italicized indicate that the corresponding protein was FRB tagged (e.g., *rrp6* = *rrp6-FRB*). The membrane was hybridized with a probe complementary to the exon 1 of *NOG2*. GAPDH was used as a loading control. E1, cleaved exon 1; Rapa, rapamycin; S, spliced mRNA; US, unspliced pre-mRNA; WT, wild type. (*B*) Northern blot analysis of *ASC1/snR191* in strains expressing FRB-tagged, AA versions of Rrp6p, Prp18p, or both Prp18p and Rrp6p. The probe used was complementary to the exon 1 of *ASC1*. ScR1 was used as a loading control. Labeling of the species is as in *A*. (*C*) Northern blot analysis of *NOG2/snR191* in strains carrying viable deletions of the genes encoding the splicing factor Lea1p and/or the RNA degradation or processing factors Dom34p, Upf1p, or Rrp6p. The probe used is complementary to the exon 1 of NOG2. ScR1 was used as a loading control. Labeling of the species is as in *A*. (*D*) Analysis of IMD4/snR54 was as described for NOG2/snR191 in *C*.

correlate with an increased accumulation of the unspliced precursors for snR191(Fig. 3*C*), suggesting that Upf1p is not involved in the conversion of unspliced precursors into hmsnoRNAs. We detected some unspliced precursor accumulation for *IMD4* in the *lea1*Δ*upf1*Δ mutant (Fig. 3*D*), but this was also detected in the *upf1*Δ mutant. While we do not fully understand the molecular basis for the decreased accumulation of hmsnoRNAs in the *lea1*Δ*upf1*Δ mutant, experiments described below using splicing signals mutations suggest that this might be the result of indirect effects. Overall, we conclude from these experiments that hmsnoRNAs are not targeted by translation-mediated RNA quality-control pathways.

hmsnoRNAs Can Be Generated by a 5′ Splice-Site Mutation and Are Degraded by the Cytoplasmic Decay Pathway Involving Xrn1p. The previous results showed that inactivation of splicing factors resulted in the accumulation of hybrid mRNA-snoRNA species. However, we could not rule out that anchoring away splicing factors or deleting genes encoding nonessential splicing factors may result in indirect effects that may hamper the interpretation of our results. To alleviate these concerns, we used a plasmid-based system to introduce splice-site mutations that would inhibit splicing and circumvent any general splicing defects. We generated a construct expressing the *NOG2-snR191* gene from a centromeric plasmid, which expressed *NOG2* at levels that exceeded the RNAs expressed from the endogenous *NOG2* gene (*SI Appendix*, Fig. S5). We did not detect any hmsnoRNA or any other aberrant species from the plasmid-borne wild-type version of *NOG2*, showing that it is fully and accurately processed (*SI Appendix*, Fig. S5). We then generated two mutants designed to inactivate splicing of the plasmid borne *NOG2* transcripts: M1 is a mutation of the 5′ splice site (SS), and M2 is a double mutation that combines M1 with a branch point (BP) mutation (Fig. 4*A*). Since the plasmid-borne versions are expressed at higher levels than the endogenous *NOG2* transcripts, and because *NOG2* is an essential gene, we used these plasmids in strains that also expressed the endogenous *NOG2* gene, which facilitated the genetic analysis. Transcripts expressed from the M1 and M2 plasmids accumulated in wild-type strains mostly as hmsnoRNAs and, to a lesser extent, as unspliced transcripts (Fig. 4*B*). The temperature used to grow strains had some influence on the level of accumulation of hmsnoRNAs derived from these mutants, as hmsnoRNAs were more abundant when cells were grown at 20 °C compared with 30 °C (*SI Appendix*, Fig. S6).

In the *rrp6*Δ mutant, the levels of hmsnoRNAs expressed from the M1 or M2 plasmids decreased with an accumulation of unspliced precursors, consistent with our previous conclusion that the nuclear exosome processes the 3′ end of hmsnoRNAs. The *dom34*Δ and *upf1*Δ mutations had no major effect on the accumulation of hmsnoRNAs expressed from these plasmids, in contrast to the result described above, which showed a decreased accumulation of hmsnoRNAs in the *lea1*Δ*upf1*Δ mutant (Fig. 3*D*). Since inactivating Upf1p does not impact the level of hmsnoRNAs generated by splicing-signal mutations, we interpret the decreased accumulation of hmsnoRNA previously observed in the *lea1*Δ*upf1*Δ mutant as the result of indirect effects. This interpretation is supported by previous work showing that mutations that reduce splicing efficiency and inactivate NMD result in synthetic growth defects (33), which may indirectly impair processes required for the accumulation of hmsnoRNAs.

In contrast to all other RNA degradation mutants analyzed previously, a large increase of all *NOG2* RNA species was detected in the *xrn1*Δ mutant deficient for the major cytoplasmic 5′-3′ exonuclease (34) (Fig. 4*B*). While the increased accumulation of spliced and unspliced species was expected, the increase in abundance of the hmsnoRNAs strongly suggests that these species are degraded in the cytoplasm by the general mRNA decay pathway, which relies primarily on Xrn1p. As hmsnoRNAs contain the 5′ ends and exon 1 sequences of the *NOG2* gene, they may contain a ^{7}meG-cap similar to that of mRNAs, which would subject them to the general decay pathway for cytoplasmic mRNAs (35). In order to show that hmsnoRNAs are degraded by the general cytoplasmic decay pathway, which requires decapping, we analyzed hmsnoRNA accumulation resulting from the M1 mutation in a strain lacking the decapping enzyme Dcp2p. As observed previously for the *xrn1*Δ mutant, inactivation of Dcp2p resulted in an increased accumulation of the hmsnoRNAs (*SI Appendix*, Fig. S7). This result is consistent with the idea that hmsnoRNAs are degraded by the major cytoplasmic decay pathway, which involves Dcp1/2-mediated decapping and 5′-3′ degradation by Xrn1p.

hmsnoRNAs Are Affected by Delocalization of Rat1p in the Cytoplasm. To test if hmsnoRNAs are affected by the nuclear 5′-3′ exonuclease Rat1p (also known as Xrn2p), we inactivated Rat1p by AA and assessed the accumulation of hmsnoRNAs from the M1 construct (Fig. 4*C*). This analysis revealed higher hmsnoRNAs levels in conditions where Rat1p is depleted from the nucleus, suggesting that a fraction of hmsnoRNAs is nuclear. It is also possible that the inactivation of Rat1p may limit

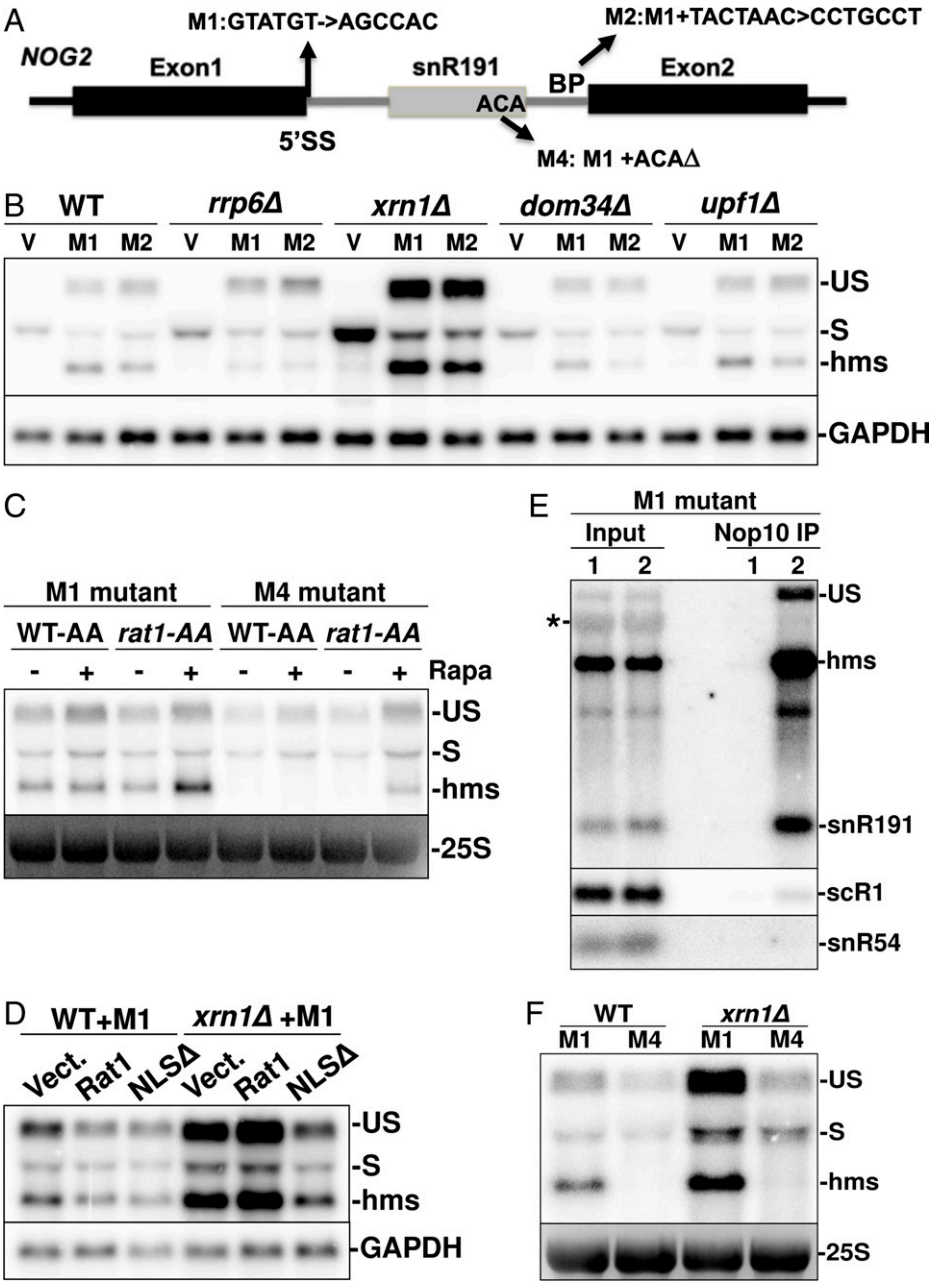

Fig. 4. hmsnoRNAs generated by SS mutations are degraded by Xrn1p and Rat1p and share some of the features of mature snoRNPs. (*A*) Mutations introduced in the plasmid expressing *NOG2-snR191*. (*B*) *NOG2-snR191* hmsnoRNAs generated by splicing signal mutations are degraded by Xrn1p but unaffected by cytoplasmic quality-control pathways. Wild-type (WT) or the indicated deletion mutants were transformed with the pUG35 vector (V) or the pUG35 plasmids expressing mutants M1 or M2, and RNAs extracted from these stains were analyzed by Northern blot using a probe hybridizing to the exon 1 of *NOG2*. GAPDH was used as a loading control. RNA species are labeled as follows: E1, cleaved exon 1; S, spliced mRNA; US, unspliced pre-mRNA. (*C*) Impact of Rat1p inactivation on hmsnoRNA levels expressed from the M1 and M4 plasmids. A WT strain or a Rat1-FRB AA strain transformed with the M1or M4 expression plasmids were grown in medium in the absence or presence of rapamycin (Rapa) for 1 h and analyzed by Northern blot as described for B. 25S rRNA was used as a loading control. (*D*) Impact of Rat1p delocalization on hmsnoRNA levels expressed from the M1 plasmid. A WT strain or an *xrn1Δ* mutant strain transformed with the M1 expression plasmid were transformed with an empty vector (vect.), a plasmid expressing WT Rat1p (Rat1), or a version of Rat1p with a mutated nuclear localization signal (NLSΔ). RNAs were analyzed by Northern blot as described for *B*. (*E*) NOG2-snR191 hmsnoRNAs generated by the M1 mutation are bound by the H/ACA snoRNP Nop10p. Shown are Northern blots of RNAs extracted from cell extracts (Input) prepared from untagged wild strain (lane 1) or ZZ-tagged Nop10 strain (lane 2) and of RNAs extracted after incubation of whole-cell extracts from the same strains with IgG beads and washing (see *Materials and Methods*). Membranes corresponding to independent purification experiments were hybridized to a probe complementary to the exon 1 of NOG2 and to snR191 (*Top*) or to probes hybridizing to scR1 or snR54 (*Bottom*). *Cross-hybridization of the probe to a ribosomal RNA. (*F*) Destabilization of hmsnoRNAs caused by the deletion of the ACA box of plasmid-borne *NOG2-snR191*s cannot be rescued by inactivation of Xrn1p. Shown is a Northern blot analysis using a probe hybridizing to the exon 1 of *NOG2* of RNAs extracted from WT or *xrn1Δ* mutants transformed with plasmids expressing the M1 or M4 constructs, as in *A*.

degradation of unspliced precursors as shown previously (25, 28), which could then be converted into hmsnoRNAs and result in higher hmsnoRNA levels.

To assess whether Rat1p could degrade hmsnoRNAs in the cytoplasm, we used plasmids expressing wild-type Rat1p or a mutant lacking its nuclear localization signal (*NLSΔ*), which was shown previously to be able to rescue Xrn1p activity (36). The expression of these constructs had little effect in a wild-type context (Fig. 4*D*). By contrast, expressing the *rat1-NLSΔ* mutant in a strain lacking Xrn1p resulted in a strong decrease

of hmsnoRNA and unspliced and mature mRNAs levels, while expressing a wild-type version of Rat1p had little impact. This result shows that a version of Rat1p, which is delocalized in the cytoplasm, can destabilize hmsnoRNAs in the absence of Xrn1p, providing further evidence that hmsnoRNAs are primarily degraded through cytoplasmic 5′-3′ decay.

hmsnoRNAs Share Some of the Hallmarks of Mature snoRNAs. The plasmid expressing *NOG2* with a mutated 5′-SS provided us a suitable system to investigate if hmsnoRNAs share some of the features of mature snoRNPs. We first asked if hmsnoRNAs are bound by a snoRNP protein found in mature snoRNPs. We performed immunoprecipitation (IP) of RNAs in a strain expressing the M1 mutant and a ZZ-tagged version of Nop10p (37), a core component of H/ACA snoRNPs. A control strain was included which did not express tagged Nop10p. Northern blot analysis of RNAs purified on immunoglobulin G (IgG) beads (which bind the ZZ-tagged Nop10p) showed that hmsnoRNAs copurified with Nop10p, as did the mature forms of *snR191* (Fig. 4*E*, IP lane 2). By contrast, non–H/ACA RNAs such as *snR54* or *scR1* were not efficiently purified (Fig. 4*E* and *SI Appendix*, Fig. S8), and no RNAs were retained on IgG beads in the strain that did not express tagged Nop10p (Fig. 4*E*, IP lane 1), showing the specificity of this immunoprecipitation procedure. The ratio of signals for the RNAs found in the Nop10p immunoprecipitates compared with the input showed very similar values for the mature snR191 and the hmsnoRNAs (*SI Appendix*, Fig. S8), suggesting that hmsnoRNAs are quantitatively bound by Nop10p. Interestingly, unspliced precursors were also immunoprecipitated by Nop10p (Fig. 4*E*). This is consistent with prior work showing cotranscriptional assembly of H/ACA snoRNPs on an intron-encoded H/ACA snoRNA in *S. cerevisiae* (38).

If hmsnoRNAs are bound by snoRNPs and stabilized by their binding, one would expect that mutation of snoRNA sequence elements that promote snoRNP assembly would result in a decrease of a steady-state levels of hmsnoRNAs, as described previously for mature H/ACA snoRNAs (1). To test this hypothesis, we generated a variant of the M1 mutant in which the ACA box of *snR191* is deleted (M4 mutant; Fig. 4*A*). This mutation resulted in the complete destabilization of the hmsnoRNA species, which were no longer detectable (Fig. 4 *C* and *F*). Strikingly, anchoring away Rat1p from the nucleus partially restored the accumulation of hmsnoRNAs expressed from this construct (Fig. 4*C*). This result shows that defective assembly of snoRNPs due to the ACA-box deletion triggers degradation of the hmsnoRNAs by nuclear 5′-3′ decay. By contrast, deletion of Xrn1p did not result in any rescue of hmsnoRNA levels from the M4 mutant, as opposed to what was observed for the hmsnoRNAs generated from the M1 construct (Fig. 4*F*). These results show that hmsnoRNAs that are not properly assembled into snoRNPs are primarily degraded by Rat1p in the nucleus and are unaffected by cytoplasmic turnover.

Discussion

In this work, we show that inactivation of splicing by impairing splicing factors or mutating splicing signals leads to the production of hybrid mRNA-snoRNA species for both box C/D or H/ACA snoRNAs. Extensive mapping of these species by Northern blot and Oxford Nanopore long-read sequencing showed that hmsnoRNA have extended 5′ ends containing mRNAs sequences that include 5′-UTR and exon 1 and that their 3′ ends match those of mature snoRNAs. This chimeric architecture is reminiscent of that of sno-lncRNAs (17), but hmsnoRNAs contain mRNA-like features instead of an snoRNA at their 5′ ends. The data we have presented suggest a general pathway for the production and degradation of hmsnoRNAs (*SI Appendix*, Fig. S9). Splicing inactivation results in accumulation of unspliced pre-mRNAs, which are bound by at least a subpopulation of snoRNPs (e.g., Nop10p for the *NOG2-snR191* hmsnoRNA) and then trimmed to or near the mature 3′ end of the snoRNA sequence by the nuclear exosome (*SI Appendix*, Fig. S9). Early binding of snoRNPs is consistent with findings of prior studies that have shown cotranscriptional assembly of snoRNP components (38–41). This assembly can occur in a splicing-independent manner (41), which explains why Nop10p can bind to hmsnoRNAs produced when splicing is inactivated (Fig. 4*E*) and why deletion of the ACA box of an *NOG2-snR191* gene containing a 5′-SS mutant significantly destabilizes the RNAs generated from this construct and triggers nuclear decay by Rat1p (Fig. 4*C*). After nuclear 3′-end processing by the exosome, hmsnoRNAs are exported to the cytoplasm, where they can be degraded by the general 5′-3′ decay pathway that involves Dcp2p and Xrn1p (*SI Appendix*, Fig. S9). Further evidence for cytoplasmic localization of hmsnoRNAs is provided by the fact that a version of Rat1p mis-localized in the cytoplasm can reduce hmsnoRNA levels in a strain lacking Xrn1p (Fig. 4*D*). Despite degradation by these 5′-3′ decay pathways, hmsnoRNA can accumulate to relatively high levels, from 10 to 64% relative to the mature snoRNA levels, depending on the snoRNA (*SI Appendix*, Table S1).

We found that inactivation of splicing factors involved at different steps of the spliceosome cycle results in the accumulation of hmsnoRNAs. This observation might be unexpected for factors involved in the second catalytic step such as Slu7p or Prp18p, as anchoring away these factors is expected to produce mostly lariat intermediates and cleaved 5′ exons but not unspliced precursors, which we showed are converted into hmsnoRNAs by the nuclear exosome. However, a recent study offers an explanation to this conundrum, as inactivation of late splicing factors can result in unspliced precursors accumulation in vivo (42), possibly because of recycling defects. Our work sheds light on previous results that described the accumulation of RNAs similar to hmsnoRNAs upon mutation of the BP sequence of the host intron of *snR18* (previously called U18) (43). The result reported in this previous study is reminiscent of the effect detected when mutating the 5′ SS and the BP of *NOG2*. In the previous study, the 5′-extended *snR18* species were interpreted as intermediates in the processing pathway (43). However, there was no evidence provided that these species could be converted into functional mature products, and based on our observations, it is more likely that they correspond to dead-end products similar to hmsnoRNAs and which are defective byproducts of splicing inactivation.

The accumulation of RNAs similar to hmsnoRNAs has also been reported when the precursor transfer RNA processing enzyme RNase P is inactivated by a thermosensitive mutation (15). These species were considered intermediates in the pathway, and their accumulation was interpreted as evidence for a direct involvement of RNase P in the processing pathway of intron-encoded snoRNAs. However, RNase P–mediated cleavage intermediates could not be detected in vivo in this study (15); furthermore, lariat introns containing snoRNAs accumulate at very high levels in a debranching enzyme mutant (10), which argues against a major cleavage pathway of intronic sequences by RNase P. We propose, instead, that the accumulation of hmsnoRNA-like RNAs in this RNase P thermosensitive mutant is, in fact, due to an indirect inhibition of splicing, as

work published later by the same group showed that this mutation results in the accumulation of unspliced pre-mRNA precursors in vivo (44), which might be converted into hmsnoRNAs.

Splicing activity has been shown to be inhibited during stress or nonstandard growth conditions (45), which suggests that hmsnoRNAs could be naturally produced in such conditions without experimental interference with the splicing process. To assess whether hmsnoRNAs might be produced in growth conditions that reduce splicing efficiency, we analyzed *NOG2* expression in stationary phase, heat-shock conditions or treatment with rapamycin (in a wild-type strain that contains a functional TOR pathway, unlike the AA strains described in *Results*). None of these conditions resulted in the accumulation of hmsnoRNAs (*SI Appendix*, Fig. S10). However, the same conditions are also known to generally reduce ribosome biogenesis and snoRNP assembly. Therefore, the absence of detection of these species in these conditions is difficult to interpret, as it might be due to conditions that globally repress ribosome biogenesis and prevent assembly of snoRNPs on the hmsnoRNA species.

The results presented here provide a general framework that underscores the importance of the splicing process for the biogenesis of snoRNAs. In the absence of splicing, not only are intron-encoded snoRNAs not processed properly but the RNAs species that are improperly generated are subject to a degradation pathway similar to that which targets mRNAs in the cytoplasm (*SI Appendix*, Fig. S9). A parallel model was proposed to underscore the importance of 5′-end processing for independently transcribed snoRNAs in *S. cerevisiae* (18). In the absence of cotranscriptional cleavage of snoRNA precursors by the endonuclease Rnt1p, unprocessed snoRNAs accumulate in the cytoplasm and are not functional (18). Overall, the results described here combined with those reported by Grzechnik et al. (18) converge to establish a unified model for the importance of RNA processing for the fate of snoRNAs. Regardless of the precise mode of expression and of the nature of the transcription units that produce snoRNAs, RNA processing of snoRNA precursors serves two major purposes: these reactions not only remove flanking sequences, they also dictate the proper fate of snoRNP particles and their mode of degradation. In the case of intron-encoded snoRNAs, the work described here establishes an additional functional role for splicing reactions beyond simply removing intervening sequences of mRNAs. Finally, these data may shed some light on the molecular effects of mutations of splicing factors, which can result in a variety of human diseases. While the impact of these mutations on mRNA splicing and alternative splicing patterns has been investigated, their effect on the production of intron-encoded snoRNAs has not been well characterized. It is possible that some of the deleterious effects of these mutations that are causal to disease may be linked to the defective processing of intron-encoded snoRNAs and the production of hmsnoRNA-like species, which may be detrimental to RNA metabolism.

Materials and Methods

Yeast strain construction and manipulation, RNA extraction, and Northern blot analysis using riboprobes were performed as described by Wang et al. (46). The list of strains, plasmids, and oligonucleotides used is provided in the *SI Appendix*. Wild-type and knockout yeast strains are from the BY4742 genetic background (47), and knockout strains were obtained from the systematic knockout collection (48). Strains used for the AA experiments are from the HHY168 genetic background (20). The detailed protocol used for direct RNA sequencing is described in detail in the *SI Appendix* and sequencing data are available at the National Center for Biotechnology Information as BioProject ID: PRJNA827814. For the expression of *NOG2* mutants, the wild-type *NOG2* gene was cloned in pUG35 (49) and expressed under the control of its own promoter to create pCL1. The M1, M2, and M4 mutants were created by site-directed mutagenesis from pCL1. For IP of ZZ-tagged Nop10p, we used strains transformed with the pFH35 plasmid that expresses ZZ-tagged Nop10p (37). RNA IP was performed as described in the *SI Appendix*.

Data Availability. Sequencing data have been deposited with the National Center for Biotechnology Information BioProject (PRJNA827814). All study data are included in the article and/or supporting information.

ACKNOWLEDGMENTS. We thank Aidan Boyne for technical help, Anthony Henras for sharing the Nop10-ZZ tagged expression plasmid and for helpful discussions, and Jeff Coller and Arlen Johnson for sharing strains and plasmids. This work was supported by the National Institute of General Medical Sciences (NIGMS; Grant R35 GM130370 to G.F.C.) M.R.G. was supported by NIGMS grant IRACDA 2K12 GM106996-06.

Author affiliations: [a]Department of Chemistry and Biochemistry, University of California, Los Angeles, CA 90095; and [b]Molecular Biology Institute, University of California, Los Angeles, CA 90095

1. A. G. Balakin, L. Smith, M. J. Fournier, The RNA world of the nucleolus: Two major families of small RNAs defined by different box elements with related functions. *Cell* **86**, 823–834 (1996).
2. J. Kufel, P. Grzechnik, Small nucleolar RNAs tell a different tale. *Trends Genet.* **35**, 104–117 (2019).
3. T. Kiss, Small nucleolar RNA-guided post-transcriptional modification of cellular RNAs. *EMBO J.* **20**, 3617–3622 (2001).
4. J. Liang *et al.*, Small nucleolar RNAs: Insight into their function in cancer. *Front. Oncol.* **9**, 587 (2019).
5. L. Faucher-Giguère, *et al.*, High-grade ovarian cancer associated H/ACA snoRNAs promote cancer cell proliferation and survival. *NAR Cancer* **4**, zcab050 (2022).
6. J. Cavaillé, Box C/D small nucleolar RNA genes and the Prader-Willi syndrome: A complex interplay. *Wiley Interdiscip. Rev. RNA* **8** e1417(2017).
7. J. E. Schaffer, Death by lipids: The role of small nucleolar RNAs in metabolic stress. *J. Biol. Chem.* **295**, 8628–8635 (2020).
8. J. W. Brown, D. F. Marshall, M. Echeverria, Intronic noncoding RNAs and splicing. *Trends Plant Sci.* **13**, 335–342 (2008).
9. T. Kiss, W. Filipowicz, Exonucleolytic processing of small nucleolar RNAs from pre-mRNA introns. *Genes Dev.* **9**, 1411–1424 (1995).
10. S. L. Ooi, D. A. Samarsky, M. J. Fournier, J. D. Boeke, Intronic snoRNA biosynthesis in *Saccharomyces cerevisiae* depends on the lariat-debranching enzyme: Intron length effects and activity of a precursor snoRNA. *RNA* **4**, 1096–1110 (1998).
11. G. Ghazal, D. Ge, J. Gervais-Bird, J. Gagnon, S. Abou Elela, Genome-wide prediction and analysis of yeast RNase III-dependent snoRNA processing signals. *Mol. Cell. Biol.* **25**, 2981–2994 (2005).
12. T. Hirose, M. D. Shu, J. A. Steitz, Splicing-dependent and -independent modes of assembly for intron-encoded box C/D snoRNPs in mammalian cells. *Mol. Cell* **12**, 113–123 (2003).
13. E. Caffarelli, M. Arese, B. Santoro, P. Fragapane, I. Bozzoni, In vitro study of processing of the intron-encoded U16 small nucleolar RNA in *Xenopus laevis*. *Mol. Cell. Biol.* **14**, 2966–2974 (1994).
14. F. Cecconi, P. Mariottini, F. Amaldi, The *Xenopus* intron-encoded U17 snoRNA is produced by exonucleolytic processing of its precursor in oocytes. *Nucleic Acids Res.* **23**, 4670–4676 (1995).
15. D. J. Coughlin, J. A. Pleiss, S. C. Walker, G. B. Whitworth, D. R. Engelke, Genome-wide search for yeast RNase P substrates reveals role in maturation of intron-encoded box C/D small nucleolar RNAs. *Proc. Natl. Acad. Sci. U.S.A.* **105**, 12218–12223 (2008).
16. G. J. S. Talross, S. Deryusheva, J. G. Gall, Stable lariats bearing a snoRNA (slb-snoRNA) in eukaryotic cells: A level of regulation for guide RNAs. *Proc. Natl. Acad. Sci. U.S.A.* **118**, e2114156118 (2021).
17. Q. F. Yin *et al.*, Long noncoding RNAs with snoRNA ends. *Mol. Cell* **48**, 219–230 (2012).
18. P. Grzechnik, *et al.*, Nuclear fate of yeast snoRNA is determined by co-transcriptional Rnt1 cleavage. *Nat. Commun.* **9**, 1–14 (2018).
19. B. S. Scruggs, C. I. Michel, D. S. Ory, J. E. Schaffer, SmD3 regulates intronic noncoding RNA biogenesis. *Mol. Cell. Biol.* **32**, 4092–4103 (2012).
20. H. Haruki, J. Nishikawa, U. K. Laemmli, The anchor-away technique: Rapid, conditional establishment of yeast mutant phenotypes. *Mol. Cell* **31**, 925–932 (2008).
21. M. C. Wahl, C. L. Will, R. Lührmann, The spliceosome: Design principles of a dynamic RNP machine. *Cell* **136**, 701–718 (2009).
22. G. Badis, M. Fromont-Racine, A. Jacquier, A snoRNA that guides the two most conserved pseudouridine modifications within rRNA confers a growth advantage in yeast. *RNA* **9**, 771–779 (2003).
23. F. Caspary, B. Séraphin, The yeast U2A′/U2B complex is required for pre-spliceosome formation. *EMBO J.* **17**, 6348–6358 (1998).
24. T. Villa, C. Guthrie, The Isy1p component of the NineTeen complex interacts with the ATPase Prp16p to regulate the fidelity of pre-mRNA splicing. *Genes Dev.* **19**, 1894–1904 (2005).
25. M. Danin-Kreiselman, C. Y. Lee, G. Chanfreau, RNAse III-mediated degradation of unspliced pre-mRNAs and lariat introns. *Mol. Cell* **11**, 1279–1289 (2003).
26. C. Allmang *et al.*, Functions of the exosome in rRNA, snoRNA and snRNA synthesis. *EMBO J.* **18**, 5399–5410 (1999).
27. K. Roy, J. Gabunilas, A. Gillespie, D. Ngo, G. F. Chanfreau, Common genomic elements promote transcriptional and DNA replication roadblocks. *Genome Res.* **26**, 1363–1375 (2016).

28. C. Bousquet-Antonelli, C. Presutti, D. Tollervey, Identification of a regulated pathway for nuclear pre-mRNA turnover. *Cell* **102**, 765–775 (2000).
29. R. K. Gudipati *et al.*, Extensive degradation of RNA precursors by the exosome in wild-type cells. *Mol. Cell* **48**, 409–421 (2012).
30. S. Sayani, G. F. Chanfreau, Sequential RNA degradation pathways provide a fail-safe mechanism to limit the accumulation of unspliced transcripts in *Saccharomyces cerevisiae*. *RNA* **18**, 1563–1572 (2012).
31. S. Meaux, A. van Hoof, K. E. Baker, Nonsense-mediated mRNA decay in yeast does not require PAB1 or a poly(A) tail. *Mol. Cell* **29**, 134–140 (2008).
32. M. K. Doma, R. Parker, Endonucleolytic cleavage of eukaryotic mRNAs with stalls in translation elongation. *Nature* **440**, 561–564 (2006).
33. T. Kawashima, M. Pellegrini, G. F. Chanfreau, Nonsense-mediated mRNA decay mutes the splicing defects of spliceosome component mutations. *RNA* **15**, 2236–2247 (2009).
34. S. Geisler, J. Coller, XRN1: A major 5′ to 3′ exoribonuclease in eukaryotic cells. *Enzymes* **31**, 97–114 (2012).
35. J. S. Mugridge, J. Coller, J. D. Gross, Structural and molecular mechanisms for the control of eukaryotic 5′-3′ mRNA decay. *Nat. Struct. Mol. Biol.* **25**, 1077–1085 (2018).
36. A. W. Johnson, Rat1p and Xrn1p are functionally interchangeable exoribonucleases that are restricted to and required in the nucleus and cytoplasm, respectively. *Mol. Cell. Biol.* **17**, 6122–6130 (1997).
37. C. Dez *et al.*, Stable expression in yeast of the mature form of human telomerase RNA depends on its association with the box H/ACA small nucleolar RNP proteins Cbf5p, Nhp2p and Nop10p. *Nucleic Acids Res.* **29**, 598–603 (2001).
38. P. K. Yang *et al.*, Cotranscriptional recruitment of the pseudouridylsynthetase Cbf5p and of the RNA binding protein Naf1p during H/ACA snoRNP assembly. *Mol. Cell. Biol.* **25**, 3295–3304 (2005).
39. M. Ballarino, M. Morlando, F. Pagano, A. Fatica, I. Bozzoni, The cotranscriptional assembly of snoRNPs controls the biosynthesis of H/ACA snoRNAs in *Saccharomyces cerevisiae*. *Mol. Cell. Biol.* **25**, 5396–5403 (2005).
40. X. Darzacq *et al.*, Stepwise RNP assembly at the site of H/ACA RNA transcription in human cells. *J. Cell Biol.* **173**, 207–218 (2006).
41. P. Richard, A. M. Kiss, X. Darzacq, T. Kiss, Cotranscriptional recognition of human intronic box H/ACA snoRNAs occurs in a splicing-independent manner. *Mol. Cell. Biol.* **26**, 2540–2549 (2006).
42. G. I. Mendoza-Ochoa, J. D. Barrass, I. E. Maudlin, J. D. Beggs, Blocking late stages of splicing quickly limits pre-spliceosome assembly in vivo. *RNA Biol.* **16**, 1775–1784 (2019).
43. T. Villa, F. Ceradini, I. Bozzoni, Identification of a novel element required for processing of intron-encoded box C/D small nucleolar RNAs in *Saccharomyces cerevisiae*. *Mol. Cell. Biol.* **20**, 1311–1320 (2000).
44. M. C. Marvin *et al.*, Accumulation of noncoding RNA due to an RNase P defect in Saccharomyces cerevisiae. *RNA* **17**, 1441–1450 (2011).
45. J. A. Pleiss, G. B. Whitworth, M. Bergkessel, C. Guthrie, Rapid, transcript-specific changes in splicing in response to environmental stress. *Mol. Cell* **27**, 928–937 (2007).
46. C. Wang *et al.*, Rrp6 moonlights in an RNA exosome-independent manner to promote cell survival and gene expression during stress. *Cell Rep.* **31**, 107754 (2020).
47. C. B. Brachmann *et al.*, Designer deletion strains derived from *Saccharomyces cerevisiae* S288C: A useful set of strains and plasmids for PCR-mediated gene disruption and other applications. *Yeast* **14**, 115–132 (1998).
48. E. A. Winzeler *et al.*, Functional characterization of the *S. cerevisiae* genome by gene deletion and parallel analysis. *Science* **285**, 901–906 (1999).
49. R. K. Niedenthal, L. Riles, M. Johnston, J. H. Hegemann, Green fluorescent protein as a marker for gene expression and subcellular localization in budding yeast. *Yeast* **12**, 773–786 (1996).